MODIFICATION OF INTERFACES IN THE GROWTH OF DIAMOND BY MW/RF PLASMA

P.REINKE, A. RAVEH*, J.E. KLEMBERG-SAPIEHA AND L. MARTINU
"Groupe de Couches Minces" and Department of Engineering Physics, École Polytechnique, Box 6079, Station A, Montréal, Québec H3C 3A7, Canada
*present address: Nuclear Research Center Negev, P.O. Box 9001, Beer-Sheva 84190, Israel

ABSTRACT

In the present work we study the growth of diamond in a dual-mode microwave/radio-frequency plasma. We investigated the effect of predeposited a-C:H films and of ion bombardment on the nucleation process and on the crystal quality. The deposits are characterized by SEM, by Raman spectroscopy and by analysis of the plasmon features in the XPS spectra.

INTRODUCTION

The development of new deposition approaches for polycrystalline diamond films has progressed significantly over the last few years, and the improvement of the material's quality has stimulated many new industrial applications /1/. However, broader use of diamond films is at present limited by their poor adhesion to numerous technologically important substrate materials. To overcome this limitation a better understanding of the nucleation process and of the interface structure is essential. Pretreatment prior to deposition is needed to optimize the initial stages of the film growth for a specific substrate material: this includes mechanical as well as chemical pretreatment, involving intermediate films, or the nucleation enhancement by additional ion bombardment /2-4/.

In the present work we study the effect of predeposited amorphous hydrogenated carbon (a-C:H) films on the nucleation and growth of diamond prepared in a microwave/radio frequency (MW/RF) plasma reactor. This system allows an independent control of processes in the principal microwave (MW) discharge and of the ion flux and ion energy at the radio-frequency (RF) powered substrate holder-electrode, where a negative dc-bias (V_B) develops /5-7/. We will discuss the influence of the thickness of a-C:H films on the nucleation density (N_D) and nucleus size distributions for different deposition conditions.The crystal quality of the deposits studied by SEM, Raman spectroscopy and XPS, is correlated to the influence of rf-biasing on the deposition.

EXPERIMENTAL

The diamond deposition was performed in a MW/RF dual frequency reactor (2.45 GHz/ 13.56 MHz), which is schematically depicted in fig. 1. The reactor consists of a waveguide, intersected by a quartz tube (19 mm in diameter), which expands to 50 mm of diameter at about 6 cm from the microwave cavity. The samples were placed in two different locations as indicated in fig. 1: (a) on a substrate holder, 3.2 cm in diameter, which could be RF-biased and seperately heated by a boron nitride heating element (position 1), and (b) inside the narrow section of the quartz tube (position 2). To expand the plasma from the small tube, a ring of permanent magnets

was installed, as illustrated in fig.1. Undoped Si (100) wafers were used as substrate material, and the typical deposition time was 2h.

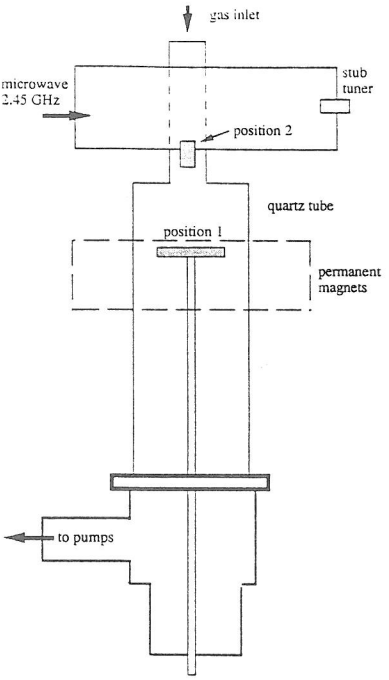

figure 1: *Schematic illustration (top view) of the MW/RF hybrid reactor used for the diamond deposition. Position 1 and 2 indicate the location of the samples. In position 1 the substrate is oriented perpendicular and in position 2 parallel with respect to the tube walls.*

The depositions in position 1 were performed in a gas mixture of 1% CH_4 diluted in H_2 at a total flow rate of 300 sccm and a pressure of 3.5 torr. A MW power of 650 W and V_B=-180 V were applied. The temperature was measured by a thermocouple in the back of the heating element, and held constant at 650°C throughout the deposition. The substrate temperature itself is estimated to exceed this value by about 150°C. The depositions at position 2 were performed without RF-biasing in a mixture of 0.7% CH_4 in H_2 at a total flow rate of 300 sccm and a pressure of 5.0 torr. The MW power was 610 W and the substrate was heated by the plasma only. The substrate temperature is estimated to be around 900°C.

The a-C:H films were deposited prior to the diamond growth in a different MW/RF reactor, described in more detail elsewhere /7/. The a-C:H films, 90, 27.4 and 14.9 nm thick, for the samples prepared in position 2 were deposited at a pressure of 100 mtorr in CH_4 and at V_B=-510 V. For the experiments at position 1 the a-C:H films, 50 and 240 nm thick, were prepared from CH_4 (17 and 50 %) in H_2 at a total pressure of 150 mtorr.

The diamond deposits were characterized by SEM (JEOL), Raman (Dilor OMARS 89) and XPS spectroscopy (VG ESCALAB-MkII). The density and size distributions of the diamond crystals were determined by optical image analysis from the SEM photographs.The thickness of the predeposited film was measured with a Sloan Dektak profilometer.

RESULTS AND DISCUSSION

The samples deposited in position 1 (see fig.1) with an applied RF-bias typically exhibit ball shaped crystals, as illustrated in fig.2a after 2 hours of growth. Although this morphology indicates the presence of large amounts of a graphitic or an amorphous phase, significant effects of the pretreatment on the nucleation can be observed. The nucleation density (N_D) was found to increase with the thickness of the a-C:H layer (d_C) from $7.3 \times 10^8 cm^{-2}$ (d_C =0 nm) to $9.0 \times 10^8 cm^{-2}$

(d_C =50 nm) and 19.4x10^8cm^{-2} (d_C =240 nm, fig. 2a). For comparison, no diamond growth has been observed for non pretreated Si substrates without RF biasing. The crystal size distribution has also been found to undergo considerable changes as it is illustrated in fig. 3c. The maximum of the distribution shifts towards larger crystal sizes and the overall number of crystals with a diameter exceeding 100 nm increases with d_C.

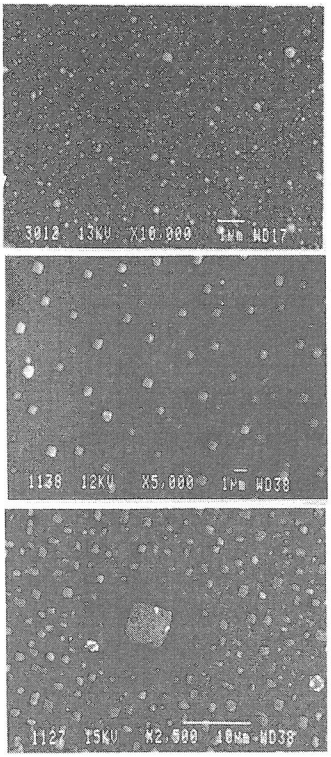

figure 2: *SEM micrographs for the following films from top to bottom: (a) film with the highest nucleation density deposited in position 1, (b) film deposited in position 2 after 1 hour with d_C=27.4 nm, and (c) shows a crystal-depleted region around a very large crystal for a film deposited in position 2 after 2 hours with d_C=90 nm.*

On the other hand the samples deposited at position 2 exhibit a quite different morphology as illustrated in fig. 2b. The crystals exhibit a rectangular or square shape, which is consistent with a (100) orientation /3/. The observed arrangement of the crystals on the surface might indicate a certain degree of heteroepitaxial growth, but this has not yet been confirmed by diffraction methods. Clearly discernible on the SEM photographs are also etch pits of similar shape as the crystals in the substrate material, and a local depletion of small nuclei around very large crystals (fig. 2c). The observed densities of the crystals are considerably smaller than those observed for the depositions at position 1, but the individual crystals are larger. The N_D values are: 0.46x10^8cm^{-2} (d_C=90 nm), 0.22 x10^8cm^{-2} (d_C=27.4 nm) and 0.48 x10^8cm^{-2} (d_C=27.4 nm) after only one hour deposition. For the thinnest a-C:H layer no growth has been observed. The size distributions for these films are shown in figs. 3a and 3b. A comparison of the samples after 1 h and 2 h of deposition (fig. 3a) shows that for a longer time crystals with a diameter of more than 1μm appear while the number of small crystals decreases considerably. We again find (fig. 3b) an increase in N_D with d_C values, but also an increase in the number of small crystals as opposed to our observation for the deposits from position 1.

Further information on the diamond and interface microstructure can be derived from the Raman spectra /8/ and XPS C1s and plasmon features /9/. The Raman spectra for the position 2 deposits, obtained by focussing on single crystals, exhibit a low intensity diamond peak against a broad peak due to the graphitic phase present. For the depositions performed in position 1 no distinct diamond peak could be observed any more but only the broad graphite peak was apparent. It has, however, to be kept in mind that the focussing

any more. The contributions of the graphitic interface layer and the large differences in the scattering cross sections for diamond and graphite make it very difficult in this case to detect small contributions of a diamond phase.

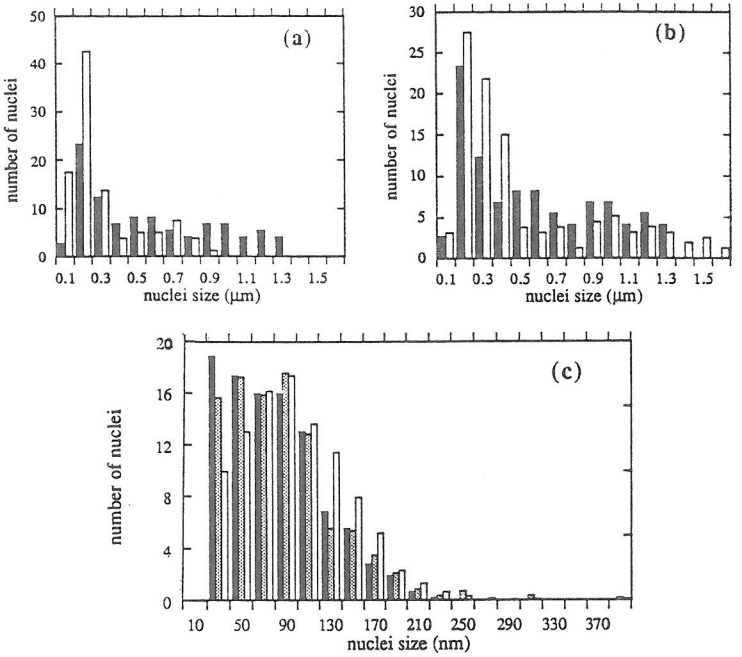

figure 3: *Normalized nuclei size distributions for films deposited at position 2: (a)□after 1 hour and ■ after 2 hours, (b) □ d_C=90 nm and ■d_C=27.4 nm, and for films deposited at position 1: (c)■ d_C=0 nm, ▣d_C=50 nm and □ d_C=240 nm.*

In the XPS spectra the C1s peak exhibits for all films contributions from the C-C bonds at 284.6 eV and from the SiC interfacial layer at 282.7 eV. However, the very small energy separation of the diamond and graphite C1s peaks of only 0.6 eV /10/ does not allow us to determine the respective contributions. The observation of the plasmon peaks, which appear on the high energy side of the main peak, is in this respect more conclusive /11/. The plasmon features for the films with the highest N_D values at both deposition positions are depicted in fig. 4. In this deconvoluted XPS spectra two prominent plasmon peaks can be distinguished: the peak centered around 31.5±0.4 eV can be associated with the diamond phase. In agreement with the Raman spectra and the SEM results this peak is much more intense for the better quality crystals of position 2 deposits. The peak at 21.0±0.3 eV, apparent in both samples, can be attributed to the graphitic phase, which is formed by annealing of the a-C:H films and the graphitic component present in the crystals . The appearance of the graphitic peak at lower energies as compared to HOPG (highly oriented pyrolytic graphite, 26 eV) is characteristic for the highly disordered

graphitic material formed by the annealing process. A third small peak at 15.2±0.7 eV has at present not been identified conclusively.

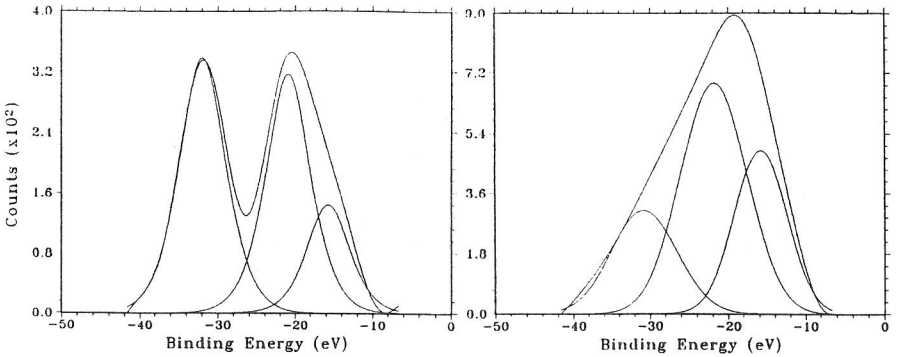

figure 4: *XPS C1s plasmon features for the films from position 1 and 2 with the highest nucleation density. The binding energies are given with respect to the C1s peak at 284.5. For comparison: the intensity of the C1s peak is about 15 times the intensity of the plasmon peak.*

When comparing the two sets of films described above most readily apparent are the differences in the crystal morphology. The poor crystallinity of the films deposited in position 1 can mainly be attributed to the ion bombardment during the film growth. The deterioration of the crystallinity is caused by the displacement of lattice atoms if the ion energies exceed the displacement threshold energy of about 50 eV /12/. On the other hand the ion bombardment can directly enhance the nucleation by contributing to the creation of active surface sites, either by the formation of graphitic clusters or surface defects. It should also be kept in mind that the application of a RF-bias leads to changes in the radical concentrations and their spatial distributions in the gas phase.

Although an increase in the nucleation density with d_C is observed for both sets of films, some differences in the size distribution of the nuclei can be found. For the depositions at position 1 the evolution of the distribution suggests that a more effective nucleation, or higher N_D, is accompanied by an acceleration of the crystal growth. The number of small crystals seems to decrease not through dissolution or etching, but by a more rapid growth, thus leading to the observed shift in the maximum of the distribution towards larger nuclei sizes after the same deposition time. The contrary is observed for the position 2 deposits. An increasing number of very small as well as very large crystals, but a depletion of the medium size region, indicates that a certain number of the small nuclei is dissolved again. A similar observation is also made for the time evolution of the distribution shown in fig 3a. The predeposited carbonaceous layer enhances the nucleation, but the local surface supersaturation of carbon atoms is not sufficient to support the rapid growth of a high number of nuclei. The growth rate is in this case limited by the surface diffusion, an assumption which is supported by the observed local depletion around very large

crystals and the decrease in the nuclei densities for a longer deposition time. The critical size above which a nucleus survives is apparently larger for the deposition conditions chosen for position 2.

CONCLUSIONS

The presence of a carbonaceous layer accelerates the formation of nuclei and contributes to an increase in the nucleation density. The consecutive growth of the crystals is to a large extent determined by the interaction with the gas phase and the available carbon supply at the surface. The RF-biasing leads, through the ion bombardment to a deterioration of the crystal quality, but it is seen to contribute to an enhancement of the nucleation density. It is at present, however, not possible to determine to what extent the increase in the plasma density in the dual-frequency mode influences the crystal growth itself. Analysis of the XPS spectra shows that a carbonaceous layer of a graphitic nature and a distinct SiC phase is present at the surface. The microstructure of this interfacial layer, which has a decisive influence on the nucleation process, has not yet been fully determined. It is not yet clear whether the carbon supersaturation, the formation of graphitic clusters or merely surface defects are the driving force for the nucleation.

ACKNOWLEDGEMENTS

This work was supported in part by the Natural Sciences and Engineering Research Council (NSERC) of Canada and by funds from Formation de Chercheurs et Aide à la Recherche (FCAR) of Québec. The DAAD (German Academic Exchange Service) is acknowledged to grant one of us (P.R.) its scholarship.

REFERENCES

/1/ P.Bachman, in Diamond and Diamond-like Films and Coatings, eds. R.E. Clausing, L.L. Horton, J.C. Angus and P.Koidl, NATO-ASI Series B:Physics **266**, 829, Plenum Press (1991)
/2/ B.R. Stoner, G.-H.M. Ma, S.D. Wolter and J.T. Glass, Phys. Rev. B **45**, 11067 (1992)
/3/ S.D. Wolter, B.R. Stoner, J.T. Glass, P.J. Ellis, D.S. Buhaenko, C.E. Jenkins and P. Southworth, Appl. Phys Lett. **62**, 1215 (1993)
/4/ P.N. Barnes and R.L.C. Wu, Appl. Phys. Lett **62**, 37 (1993)
/5/ L. Martinu, J.E. Klemberg-Sapieha and M.R. Wertheimer, Appl. Phys. Lett **54**, 2645 (1989)
/6/ J.E. Klemberg-Sapieha, O.M. Küttel, L. Martinu and M.R. Wertheimer, Thin Solid Films **193/194**, 965 (1990)
/7/ L. Martinu, A. Raveh, A. Domingue, L. Bertrand, J.E. Klemberg-Saphieha, S.C. Gujrathi and M.R. Wertheimer, Thin Solid Films **208**, 42 (1992)
/8/ P.K. Bachmann and D.U. Wiechert, in Diamond and Diamond-like Films and Coatings, eds. R.E. Clausing, L.L. Horton, J.C. Angus and P.Koidl, NATO-ASI Series B:Physics **266**, 677, Plenum Press (1991)
/9/ D.N. Belton, S.J. Harris, S.J. Schmieg, A.M. Weiner and T.A. Perry, Appl. Phys. Lett. **54**, 416 (1989)
/10/ J.J. Cuomo, J.P. Doyle, J. Bruley and J.C. Lui, Appl. Phys. Lett. **58**, 466 (1991)
/11/ J. Fink, Th. Müller-Heinzerling, J. Pflüger, B. Scheerer, B. Dischler, P. Koidl, A. Bubenzer and R.E. Sah, Phys. Rev B **30**, 4713 (1984)
/12/ J. Koike, D.M. Parkin and T.E. Mitchell, Appl. Phys. Lett. **60**, 1450 (1992)